

# EvoMail: Self-Evolving Cognitive Agents for Adaptive Spam and Phishing Email Defense

Wei Huang<sup>1\*</sup> De-Tian Chu<sup>2\*</sup> Lin-Yuan Bai<sup>2</sup> Wei Kang<sup>2</sup> Hai-Tao Zhang<sup>2</sup> Bo Li<sup>2</sup>  
 Zhi-Mo Han<sup>3</sup> Jing Ge<sup>2</sup> Hai-Feng Lin<sup>2†</sup>

<sup>1</sup> People's Liberation Army 77606 Unit, Lasa 850000, China

<sup>2</sup> Field Engineering College, Army Engineering University of PLA, Nanjing 210007, China

<sup>3</sup> College Of Software, ZhengZhou University of Light Industry, Zhengzhou 450000, China

hwazyx2013@163.com, Detian\_chu@aeu.edu.cn, linyuan\_bai@aeu.edu.cn,  
 w\_kang2023@163.com, kirby8zhang@163.com, 13999932025@163.com,  
 542313460107@zzuli.edu.cn, 19822649042@163.com

## Abstract

Modern email spam and phishing attacks have evolved far beyond keyword blacklists or simple heuristics, now focusing on complex intent exploitation that traditional systems struggle to understand (Wang et al. 2025b). Adversaries now craft multi-modal campaigns that combine natural-language text with obfuscated URLs, forged headers, and malicious attachments, adapting their strategies within days to bypass filters (Lin et al. 2021)(Wang et al. 2025a). Traditional spam detection systems, which rely on static rules or single-modality models, struggle to integrate heterogeneous signals or to continuously adapt, leading to rapid performance degradation.

We propose EvoMail, a self-evolving cognitive agent framework for robust detection of spam and phishing, building on recent advances in agent-based systems with memory and reflection capabilities (Zhou et al. 2024b)(Liang et al. 2025). EvoMail first constructs a unified heterogeneous email graph that fuses textual content, metadata (headers, senders, domains), and embedded resources (URLs, attachments). A Cognitive Graph Neural Network (COGGNN) enhanced by a Large Language Model (LLM) performs context-aware reasoning across these sources to identify coordinated spam campaigns. Most critically, EvoMail engages in an adversarial self-evolution loop: a “red-team” agent generates novel evasion tactics—such as character obfuscation or AI-generated phishing text (Li et al. 2020)—while the “blue-team” detector learns from failures, compresses experiences into a memory module (Zhou et al. 2024b), and reuses them for future reasoning.

Extensive experiments on real-world datasets (Enron-Spam, Ling-Spam, SpamAssassin, and TREC) and synthetic adversarial variants demonstrate that EvoMail consistently outperforms state-of-the-art baselines in detection accuracy, adaptability to evolving spam tactics, and interpretability of reasoning traces. These results highlight EvoMail’s potential as a resilient and explainable defense framework against next-generation spam and phishing threats.

## Introduction

Email remains a universal communication backbone but also the primary vector for spam and phishing (Goenka, Chawla, and Tiwari 2024). Contemporary campaigns are *multi-source and rapidly adaptive* (Rossi et al. 2020): natural and fluent text, obfuscated or shortened URLs, forged headers (SPF/DKIM/DMARC evasions), and polymorphic attachments. As filters are updated, attackers leverage powerful generative models (Liu et al. 2025) to mutate content within days via prompt-engineering or template-based generation. Traditional rule-based or single-modality classifiers (Xiong et al. 2024) (e.g., keyword lists, Naive Bayes) perform well on known patterns but generalize poorly under tactic drift.

Advanced neural methods have improved robustness, yet three gaps persist: (i) **Heterogeneous fusion**: indicators span text, headers, domains, and attachments; modeling subtle cross-modal correlations (Wang et al. 2024b) (Li et al. 2023a) remains challenging (Wang et al. 2025a) (Xin et al. 2024b). (ii) **Adaptation**: distribution shifts (Li et al. 2023c) from obfuscation, domain rotation, and AI-generated content quickly erode static models, a challenge addressed by recent domain adaptation methods (Wang et al. 2024a) (Kirkpatrick et al. 2017) (Du et al. 2024). (iii) **Contextual memory**: detectors rarely retain and reuse reasoning traces (Li et al. 2023c) (Lyu et al. 2025), limiting recognition of variants of previously observed attacks.

We present **COG**, a self-evolving cognitive agent that mimics human analysts (Ren et al. 2024) (Li et al. 2023b). COG unifies multi-source signals into a heterogeneous email graph and applies an LLM-enhanced **COGGNN** for semantic-structural reasoning. A *red-blue* adversarial loop continuously surfaces novel evasion tactics (Li et al. 2023a) and converts detection failures into compressed, reusable experiences, injected back into reasoning and fine-tuning. Our contributions:

- **Self-evolving agent for spam/phishing:** a closed-loop framework combining heterogeneous email graphs (Li et al. 2024), LLM-augmented GNN reasoning, adver-

\*Equal contribution.

†Corresponding author: hfliing@compintel.cn

Copyright © 2025, Association for the Advancement of Artificial Intelligence (www.aaai.org). All rights reserved.

serial generation, and experience compression(Li et al. 2024).

- **COGGNN:** an LLM-guided semantic attention and query optimizer that couples textual semantics with graph structure across content, headers, domains, and attachments.
- **Experience compression & reuse:** distills failed traces into structured heuristics to stabilize adaptation under distributional and adversarial shifts.
- **Comprehensive evaluation:** static, shift, and cross-modal settings on public corpora and synthetic adversarial variants; we report accuracy/F1 as well as STC (structured temporal consistency) and CIM (cognitive interpretability) for regulator-aligned transparency.

## Related Work

**Email spam and phishing detection.** Classical filters (Bayes(Metsis, Androutsopoulos, and Palioras 2006), SVM(Fette, Sadeh, and Tomasic 2007), rule lists) and modern neural models (TextCNN(Kim 2014), Transformers) predominantly focus on content, with metadata and URLs often auxiliary. Graph-based perspectives connect senders, recipients, domains, and URLs but struggle to fuse semantics and structure end-to-end. (Wu et al. 2021) (Li et al. 2025)(Schlichtkrull et al. 2017)

**LLMs for security text.** LLMs excel at contextual reasoning and pattern abstraction, and have been successfully applied to tasks like phishing email detection(Devlin et al. 2019)(Brown et al. 2020)(Zhao et al. 2025); yet without persistent memory and guardrails, they can be brittle to prompt injection or novel obfuscation(Wei, Haghtalab, and Steinhardt 2023)(Zhou et al. 2024a), and their inference efficiency remains a consideration (Wan et al. 2025b). Integrating LLMs with structured models (graphs(Zhao et al. 2023)(Ede et al. 2022)) is a promising path(Wan et al. 2025a) toward richer evidence aggregation(Liang, Ding, and Fu 2021)(Qian et al. 2023).

**Self-evolving systems.** Self-play(Silver et al. 2016), reflective memory, and inference-time optimization through reflection (Zhuo et al. 2025) have shown promise in dynamic domains, alongside online prompt/model updates(Xin et al. 2024a) for tasks ranging from game playing to automated cyber defense(Palmer et al. 2024). For email security, realizing safe, auditable, and data-efficient self-evolution remains under-explored(Zhou et al. 2024a)(Thapa et al. 2023).

## Problem Formulation

Let  $\mathcal{D} = \{D^{\text{text}}, D^{\text{meta}}, D^{\text{url}}, D^{\text{att}}\}$  denote email content, metadata (headers/senders/receivers/domains), URLs, and attachments. We build a heterogeneous graph  $G = (V, E, X)$  with node types (emails, senders, receivers, domains, URLs, attachments) and relation types (sent\_to, hosted\_on, contains, linked\_to, replied\_to) (Wang et al. 2021). Each node  $v \in V$  has features  $x_v$  (e.g., text embeddings, header signals, URL features, file hashes/MIME).

Given an email (or email thread)  $q$ , the task is to predict  $y \in \{0, 1\}$  (ham vs. spam/phishing):

$$\hat{y} = f_\theta(q, G) \in [0, 1], \quad (1)$$

where  $f_\theta$  integrates local content and global graph context.

## Method: COG Framework

### Overview

Figure 1 provides an overview of the COG framework. Incoming emails are represented as nodes of different types (emails, senders, recipients, domains, URLs, attachments), with edges capturing semantic and structural relations such as sent\_to, contains, hosted\_on, and linked\_to. These nodes and edges together form a heterogeneous email graph, over which the LLM-enhanced CogGNN performs multi-source reasoning. Highlighted edges in the figure indicate a high-attention *evidence path*, showing how EvoMail aggregates suspicious cues—e.g., forged headers, anomalous domains, or obfuscated URLs—into an interpretable reasoning trace that explains why an email is classified as spam or phishing. The full framework integrates four modules: (1) heterogeneous graph construction, (2) CogGNN reasoning with LLM-guided attention, (3) self-evolution via red–blue adversarial training and experience compression(Khosla, Zhu, and He 2023), and (4) explainable evidence-path backtracing.

### Notation and Definitions

We summarize the notation used throughout this section:

- $G = (\mathcal{V}, \mathcal{E}, \mathcal{R})$ : heterogeneous email graph with nodes  $\mathcal{V}$ , edges  $\mathcal{E}$ , and relation types  $\mathcal{R}$ .
- $v_i \in \mathcal{V}$ : email node  $i$  with raw feature vector  $x_i \in \mathbb{R}^d$ .
- $h_v^{(0)} \in \mathbb{R}^{d_h}$ : initial embedding of node  $v$  after feature transformation.
- $h_v^{(k)} \in \mathbb{R}^{d_h}$ : hidden representation of node  $v$  at GNN layer  $k \in \{1, \dots, L\}$ .
- $\mathcal{N}(v)$ : full neighborhood of node  $v$ ;  $\mathcal{N}_K(v) \subseteq \mathcal{N}(v)$ : top- $K$  selected neighbors.
- $e_{uv} \in \mathcal{E}$ : edge between nodes  $u$  and  $v$  with relation type  $r_{uv} \in \mathcal{R}$ .
- $\alpha_{uv}^{(k)} \in [0, 1]$ : attention weight from node  $u$  to  $v$  at layer  $k$ .
- $f_\theta : \mathbb{R}^d \rightarrow [0, 1]$ : detection model parameterized by  $\theta$ .
- $\mathcal{M}_t$ : compressed memory at iteration  $t$ , storing tuples  $(e, \hat{y}, \text{trace})$ .
- $\mathcal{A}_t = \{E_{\text{adv}}^{(m)}\}_{m=1}^{M_t}$ : set of adversarial samples at iteration  $t$ .
- $\phi : \mathcal{V} \rightarrow \mathbb{R}^{d_\phi}$ : feature extraction function mapping emails to embedding space.
- $P(u, v) \in \mathbb{R}^{d_p}$ : contextualized prompt embedding for node pair  $(u, v)$ .
- Hyperparameters:  $K$  (neighbors),  $L$  (GNN layers),  $\tau$  (temperature),  $\beta$  (balance),  $\lambda, \mu$  (loss weights),  $M_{\max}$  (memory budget).

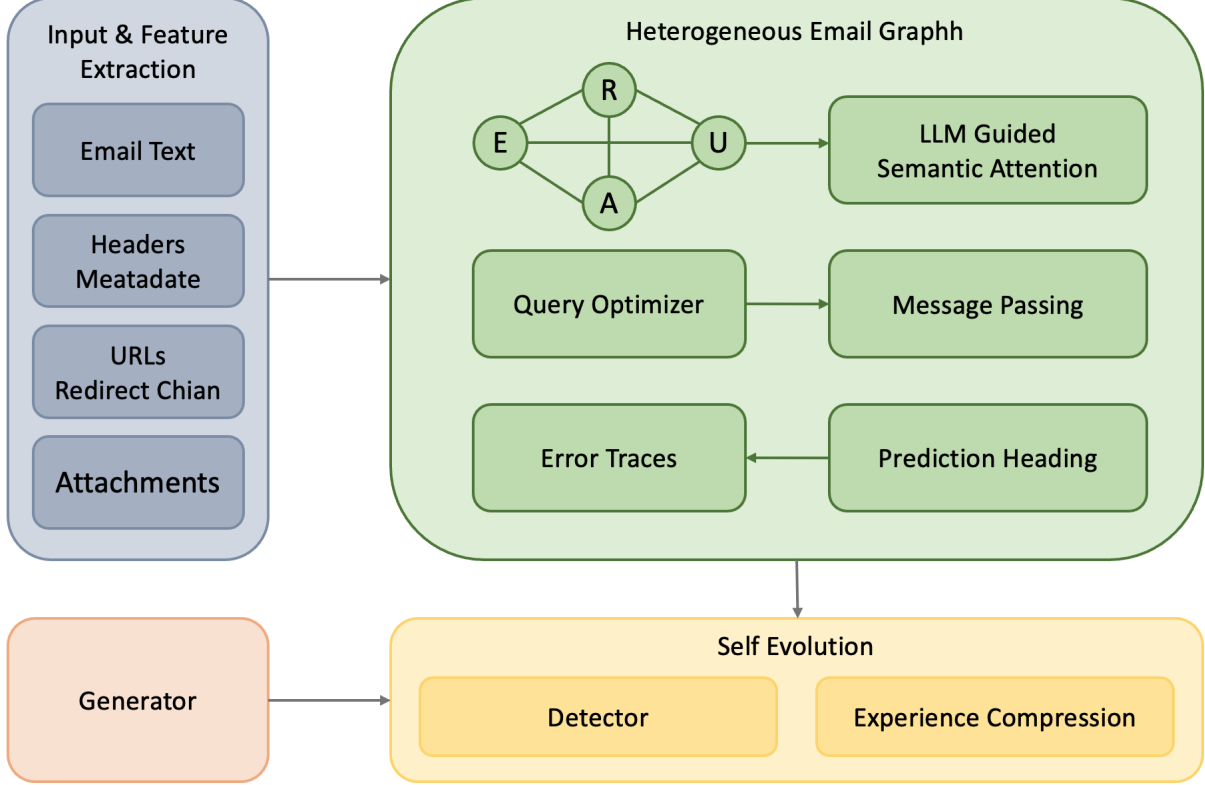


Figure 1: Schematic: heterogeneous email graph and high-attention evidence path .

## Heterogeneous Graph Construction

**Multi-modal feature extraction.** For each email  $v$ , we extract features from multiple modalities and construct the initial representation:

$$x_v^{\text{text}} = \text{TF-IDF}(\text{subject}(v)) \oplus \text{TF-IDF}(\text{body}(v)) \in \mathbb{R}^{d_t}, \quad (2)$$

$$x_v^{\text{meta}} = \begin{bmatrix} \text{hour}(v), \text{weekday}(v), \\ \text{length}(v), \text{attach\_count}(v) \end{bmatrix} \in \mathbb{R}^{d_m}, \quad (3)$$

$$x_v^{\text{network}} = \begin{bmatrix} \text{sender\_rep}(v), \text{domain\_age}(v), \\ \text{url\_count}(v) \end{bmatrix} \in \mathbb{R}^{d_n}, \quad (4)$$

$$x_v = x_v^{\text{text}} \oplus x_v^{\text{meta}} \oplus x_v^{\text{network}} \in \mathbb{R}^d \quad (5)$$

where  $\oplus$  denotes vector concatenation,  $d = d_t + d_m + d_n$ , and each component captures different aspects of email characteristics.

**Relation modeling.** We define multiple relation types in  $\mathcal{R} = \{r_1, r_2, \dots, r_{|\mathcal{R}|}\}$ :

$$r_{\text{domain}}(u, v) = \mathbb{I}[\text{domain}(u) = \text{domain}(v)] \cdot w_{\text{domain}}, \quad (6)$$

$$r_{\text{temporal}}(u, v) = \exp\left(-\frac{|\text{timestamp}(u) - \text{timestamp}(v)|}{\sigma_t}\right) \cdot w_{\text{temporal}} \quad (7)$$

$$r_{\text{semantic}}(u, v) = \cos(\text{BERT}(u), \text{BERT}(v)) \cdot w_{\text{semantic}}, \quad (8)$$

$$r_{\text{sender}}(u, v) = \mathbb{I}[\text{sender}(u) = \text{sender}(v)] \cdot w_{\text{sender}} \quad (9)$$

where  $\mathbb{I}[\cdot]$  is the indicator function,  $\sigma_t > 0$  controls temporal decay, and  $w_{\text{type}} > 0$  are learned relation weights.

**Edge construction.** An edge  $e_{uv}$  exists if any relation exceeds threshold  $\epsilon_r$ :

$$e_{uv} \in \mathcal{E} \iff \max_{r \in \mathcal{R}} r(u, v) > \epsilon_r, \quad \text{with weight } W_{uv} = \sum_{r \in \mathcal{R}} r(u, v). \quad (10)$$

## CogGNN: LLM-Enhanced Cognitive Graph Neural Network

**Initial embedding transformation.** Raw features are transformed into hidden space via learnable projection:

$$h_v^{(0)} = \text{LayerNorm}(\sigma(W_{\text{init}}x_v + b_{\text{init}})) \in \mathbb{R}^{d_h} \quad (11)$$

where  $W_{\text{init}} \in \mathbb{R}^{d_h \times d}$ ,  $b_{\text{init}} \in \mathbb{R}^{d_h}$ , and  $\sigma(\cdot)$  is the ReLU activation.

**Contextual prompt generation.** For each node pair  $(u, v)$ , we construct a structured prompt and encode it:

$$\text{prompt\_str}(u, v) = \text{TEMPLATE}\left(\text{desc}(u), \text{desc}(v), \text{relation}(e_{uv}), \text{task\_context}\right), \quad (12)$$

$$P(u, v) = \text{LLM}_{\text{encoder}}(\text{prompt\_str}(u, v)) \in \mathbb{R}^{d_p} \quad (13)$$

where  $\text{LLM}_{\text{encoder}}$  produces contextualized embeddings capturing semantic relationships.

**Adaptive neighbor selection.** We compute a composite salience score integrating multiple signals:

$$s_{\text{struct}}(u, v) = \text{PageRank}(u) + \frac{\deg(u)}{\max_i \deg(v_i)}, \quad (14)$$

$$+ \frac{1}{1 + \text{shortest\_path}(u, v)}$$

$$s_{\text{freq}}(u, v) = \frac{\text{co\_occurrence}(u, v)}{\sqrt{\text{total\_count}(u) \cdot \text{total\_count}(v)}}, \quad (15)$$

$$s_{\text{semantic}}(u, v) = \frac{h_u^{(0)} \cdot h_v^{(0)}}{\|h_u^{(0)}\|_2 \|h_v^{(0)}\|_2}, \quad (16)$$

$$S(u, v) = w_s \cdot s_{\text{struct}}(u, v) + w_f \cdot s_{\text{freq}}(u, v) + w_c \cdot s_{\text{semantic}}(u, v) \quad (17)$$

$$(18)$$

where  $[w_s, w_f, w_c] = \text{softmax}([a_s, a_f, a_c])$  with learnable parameters  $a_s, a_f, a_c \in \mathbb{R}$ . The top- $K$  neighbors are selected as:

$$\mathcal{N}_K(v) = \{u_1, u_2, \dots, u_K\}$$

$$\text{where } S(u_1, v) \geq S(u_2, v) \geq \dots \geq S(u_K, v). \quad (19)$$

**LLM-guided attention mechanism.** Building upon the principles of graph attention networks(Veličković et al. 2018), for each layer  $k$ , attention weights integrate semantic and structural reasoning(Chen et al. 2025):

$$\text{llm\_score}(u, v) = \text{MLP}_{\text{attn}}(P(u, v)) \in [0, 1], \quad (20)$$

$$\text{struct\_features}(u, v) = [w_r^\top \text{onehot}(r_{uv}), \log(1 + \deg(u)), \log(1 + \deg(v)), \frac{1}{1 + \text{spath}(u, v)}] \quad (21)$$

$$\text{struct\_score}(u, v) = w_{\text{struct}}^\top \text{struct\_features}(u, v), \quad (22)$$

$$e_{uv}^{(k)} = \text{llm\_score}(u, v) + \beta \cdot \text{struct\_score}(u, v),$$

$$+ \gamma \cdot \frac{h_u^{(k-1)} \cdot h_v^{(k-1)}}{\|h_u^{(k-1)}\|_2 \|h_v^{(k-1)}\|_2} \quad (23)$$

$$\alpha_{uv}^{(k)} = \frac{\exp(e_{uv}^{(k)} / \tau)}{\sum_{j \in \mathcal{N}_K(v)} \exp(e_{jv}^{(k)} / \tau)} \quad (24)$$

where  $\text{MLP}_{\text{attn}}$  is a multi-layer perceptron,  $w_r \in \mathbb{R}^{|\mathcal{R}|}$  are relation embedding weights,  $w_{\text{struct}} \in \mathbb{R}^4$ , and  $\gamma \geq 0$  controls the influence of current representations.

**Multi-layer message passing.** Node representations evolve through  $L$  layers of message aggregation:

$$m_v^{(k)} = \sum_{u \in \mathcal{N}_K(v)} \alpha_{uv}^{(k)} \cdot (W_{\text{neigh}}^{(k)} h_u^{(k-1)} + W_{\text{edge}}^{(k)} \text{embed}(r_{uv})), \quad (25)$$

$$\tilde{h}_v^{(k)} = W_{\text{self}}^{(k)} h_v^{(k-1)} + m_v^{(k)} + b^{(k)}, \quad (26)$$

$$h_v^{(k)} = \text{LayerNorm}(\sigma(\tilde{h}_v^{(k)})) + \text{Dropout}(h_v^{(k-1)}) \quad (27)$$

where  $W_{\text{neigh}}, W_{\text{self}}, W_{\text{edge}} \in \mathbb{R}^{d_h \times d_h}$  are layer-specific transformation matrices,  $\text{embed}(r_{uv}) \in \mathbb{R}^{d_h}$  embeds relation types, and we include residual connections for training stability(He et al. 2015).

**Final prediction.** The detection score combines multi-layer representations:

$$z_v = \text{Concat}([h_v^{(1)}, h_v^{(2)}, \dots, h_v^{(L)}]) \in \mathbb{R}^{L \cdot d_h}, \quad (28)$$

$$\hat{y}_v = \text{sigmoid}(W_{\text{out}} z_v + b_{\text{out}}) \quad (29)$$

where  $W_{\text{out}} \in \mathbb{R}^{1 \times L \cdot d_h}$  and  $b_{\text{out}} \in \mathbb{R}$ .

## Self-Evolution via Red-Blue Adversarial Training

**Red team: Adversarial sample generation.** The red team generates adversarial emails through gradient-based and semantic perturbations(Goodfellow, Shlens, and Szegedy 2015)(Ganguli et al. 2022):

$$E_{\text{grad}} = E_{\text{seed}} + \epsilon \cdot \text{sign}(\nabla_{E_{\text{seed}}} \log f_\theta(E_{\text{seed}})), \quad (30)$$

$$E_{\text{semantic}} = \text{SemanticMutate}(E_{\text{seed}}, \mathcal{V}_{\text{vocab}}, \rho_{\text{mut}}), \quad (31)$$

$$E_{\text{hybrid}} = \text{Combine}(E_{\text{grad}}, E_{\text{semantic}}, \lambda_{\text{hybrid}}) \quad (32)$$

where  $\epsilon > 0$  controls perturbation magnitude,  $\mathcal{V}_{\text{vocab}}$  is the vocabulary for semantic mutations,  $\rho_{\text{mut}} \in [0, 1]$  is mutation rate, and  $\lambda_{\text{hybrid}} \in [0, 1]$  balances the combination.

The red team optimizes a multi-objective reward:

$$\text{Novelty}(E_{\text{adv}}) = \min_{(e_i, \hat{y}_i, t_i) \in \mathcal{M}_t} \|\phi(E_{\text{adv}}) - \phi(e_i)\|_2, \quad (33)$$

$$\text{Evasion}(E_{\text{adv}}) = \max(0, 0.5 - f_\theta(E_{\text{adv}})), \quad (34)$$

$$\text{Complexity}(E_{\text{adv}}) = \frac{\|\phi(E_{\text{adv}}) - \phi(E_{\text{seed}})\|_2}{\|\phi(E_{\text{seed}})\|_2}, \quad (35)$$

$$R_{\text{red}}(E_{\text{adv}}) = w_n \cdot \text{Novelty}(E_{\text{adv}}) + w_e \cdot \text{Evasion}(E_{\text{adv}}) - w_c \cdot \text{Complexity}(E_{\text{adv}}) \quad (36)$$

where  $w_n + w_e + w_c = 1$  and  $w_n, w_e, w_c \geq 0$ .

**Blue team: Failure analysis.** The blue team detects failures and extracts detailed traces:

$$\mathcal{F}_t = \{E \in \mathcal{A}_t : f_\theta(E) < \delta_{\text{fail}} \text{ and } \text{ground\_truth}(E) = 1\}, \quad (37)$$

$$\text{Trace}(E_{\text{fail}}) = \{h_v^{(k)}, \{\alpha_{uv}^{(k)}\}_{u \in \mathcal{N}_K(v)}, \text{path}(v)\}_{k=1}^L \quad (38)$$

where  $\delta_{\text{fail}} = 0.5$  is the failure threshold and  $\text{path}(v)$  records the attention-based reasoning path.

**Experience compression and memory management(Lopez-Paz and Ranzato 2022).** Failed traces are clustered and compressed using  $k$ -medoids:

$$\text{dist}(E_1, E_2) = \|\phi(E_1) - \phi(E_2)\|_2 + \alpha_{\text{trace}} \cdot \text{trace\_dist}(\text{Trace}(E_1), \text{Trace}(E_2)), \quad (39)$$

$$\mathcal{C} = \text{KMedoids}(\mathcal{F}_t, k_t), \quad (40)$$

$$k_t = \min(|\mathcal{F}_t|, M_{\max} - |\mathcal{M}_t|)$$

$$\tilde{e}_j = \arg \min_{e \in \mathcal{C}_j} \sum_{e' \in \mathcal{C}_j} \text{dist}(e, e'), \quad (41)$$

$$\mathcal{M}_{t+1} = \text{LRU} \left( \mathcal{M}_t \cup \{(\tilde{e}_j, f_{\theta_t}(\tilde{e}_j), \text{Trace}(\tilde{e}_j))\}_{j=1}^{|\mathcal{C}|}, M_{\max} \right) \quad (42)$$

where  $\alpha_{\text{trace}} \geq 0$  weights trace similarity, and LRU removes oldest entries when memory exceeds capacity.

**Adversarial training objective.** The total loss integrates task performance, memory consistency, and adversarial robustness:

$$\mathcal{L}_{\text{task}}(\theta) = - \sum_{(v, y) \in \mathcal{D}} [y \log f_{\theta}(v) + (1 - y) \log(1 - f_{\theta}(v))], \quad (43)$$

$$\mathcal{L}_{\text{cons}}(\theta) = - \sum_{(e, \hat{y}, t) \in \mathcal{M}_t} [\hat{y} \log f_{\theta}(e) + (1 - \hat{y}) \log(1 - f_{\theta}(e))], \quad (44)$$

$$\mathcal{L}_{\text{adv}}(\theta) = - \sum_{E \in \mathcal{A}_t} \log f_{\theta}(E) + \sum_{E \in \mathcal{A}_t} \log(1 - f_{\theta}(E_{\text{benign}})), \quad (45)$$

$$\mathcal{L}_{\text{reg}}(\theta) = \|\theta\|_2^2, \quad (46)$$

$$\mathcal{L}_{\text{total}}(\theta) = \mathcal{L}_{\text{task}}(\theta) + \lambda \mathcal{L}_{\text{cons}}(\theta) + \mu \mathcal{L}_{\text{adv}}(\theta) + \nu \mathcal{L}_{\text{reg}}(\theta) \quad (47)$$

where  $E_{\text{benign}}$  are benign emails, and  $\nu > 0$  controls regularization strength.

## Explainable Reasoning

To ensure transparency and auditability, a critical requirement for security applications, we develop an explainable reasoning module(Ribeiro, Singh, and Guestrin 2016)(Lundberg and Lee 2017). Our explanation approach, which extracts the most influential evidence path, is one of several paradigms in graph explainability(Vu and Thai 2020). It contrasts with counterfactual methods that identify minimal changes to flip a prediction, and with probabilistic approaches that generate a distribution over explanatory subgraphs. Furthermore, it differs from decomposition-based methods like Layer-wise Relevance Propagation (LRP)(Bach et al. 2015), which explain predictions by propagating relevance scores backwards through the network.

**Evidence path extraction with confidence scoring.** Similar to methods developed for explaining GNNs(Ying et al.

2019), we extract reasoning paths by following high-attention edges with confidence assessment:

$$\text{confidence}(v, k) = \max_{u \in \mathcal{N}_K(v)} \alpha_{uv}^{(k)}, \quad (48)$$

$$u_i^* = \arg \max_{u \in \mathcal{N}_K(u_{i-1}^*)} \alpha_{u, u_{i-1}^*}^{(L-i+1)}, \quad (49)$$

$$\begin{aligned} \text{Path}(v) = & [(v, \text{confidence}(v, L)), \\ & (u_1^*, \text{confidence}(u_1^*, L-1)), \dots, \\ & (u_d^*, \text{confidence}(u_d^*, L-d))] \end{aligned} \quad (50)$$

where path extraction stops when  $d \geq D_{\max}$  or  $\text{confidence}(u_d^*, L-d) < \alpha_{\min}$ .

**Feature importance scoring.** For each node in the reasoning path, we compute feature importance via gradient analysis:

$$\text{importance}(f_i, v) = \left| \frac{\partial f_{\theta}(v)}{\partial x_{v,i}} \right| \cdot |x_{v,i}|, \quad (51)$$

$$\text{top\_features}(v) = \text{TopK}_i(\text{importance}(f_i, v), K_{\text{feat}}) \quad (52)$$

where  $x_{v,i}$  is the  $i$ -th feature of node  $v$  and  $K_{\text{feat}}$  controls the number of important features to report.

**Natural language explanation generation(Lucic et al. 2022).** Explanations combine path analysis with feature importance:

$$\begin{aligned} \text{path\_summary} = & \text{SUMMARIZE} \left( \{(\text{type}(u_i), \right. \\ & \left. \text{relation}(u_i, u_{i-1}), \text{confidence}(u_i))\}_{i=1}^d \right) \end{aligned} \quad (53)$$

$$\text{feature\_summary} = \text{DESCRIBE} \left( \bigcup_{i=1}^d \text{top\_features}(u_i) \right), \quad (54)$$

$$\begin{aligned} \text{Explanation}(v) = & \text{TEMPLATE} \left( \text{path\_summary}, \right. \\ & \left. \text{feature\_summary}, f_{\theta}(v) \right) \end{aligned} \quad (55)$$

## Theoretical Analysis

**Theorem 1** (Convergence Guarantee). *Assume each loss component in  $\mathcal{L}_{\text{total}}$  is  $L$ -Lipschitz continuous with respect to  $\theta$ . If the learning rate satisfies  $\eta \leq 1/(2L)$ , then gradient descent converges to an  $\epsilon$ -stationary point in  $O(1/\epsilon^2)$  iterations.*

*Sketch.* The weighted sum of Lipschitz functions remains Lipschitz with constant  $L_{\text{total}} = L + \lambda L + \mu L + \nu L = (1 + \lambda + \mu + \nu)L$ . Standard analysis of non-convex optimization (Ghadimi and Lan 2013) shows that  $\mathbb{E}[\|\nabla \mathcal{L}_{\text{total}}\|^2]$  decreases at rate  $O(1/T)$ .  $\square$

**Theorem 2** (Per-layer Time Complexity of COGGNN). *Let  $|\mathcal{V}|$  be the number of nodes,  $L$  the number of layers,  $K$  the Top- $K$  neighbors per node,  $H$  the number of attention heads, and  $d_h$  the head (or hidden) dimension. Let  $C_{\text{LLM}}$  denote the cost of invoking the LLM on a node–neighbor pair. Assuming sparse neighborhoods (max degree absorbed into*

Algorithm 1: COG Framework Training

---

**Require:** Dataset  $\mathcal{D}$ , hyperparameters  $\{K, L, \lambda, \mu, \nu, \eta, M_{\max}\}$

- 1: Initialize parameters  $\theta$ , memory  $\mathcal{M}_0 = \emptyset$
- 2: Construct heterogeneous graph  $\mathcal{G}$  using Equations
- 3: **for**  $t = 1$  to  $T$  **do**
- 4:   // Forward pass with current model
- 5:   Compute predictions  $\{\hat{y}_v\}_{v \in \mathcal{V}}$  using Equations
- 6:   // Red team adversarial generation
- 7:    $\mathcal{A}_t \leftarrow \text{REDTEAM.GENERATE}(f_\theta, \mathcal{M}_t)$  using Equations
- 8:   // Blue team failure detection
- 9:    $\mathcal{F}_t \leftarrow \text{BLUETEAM.FAILURES}(\mathcal{A}_t, f_\theta)$  using Equations
- 10:   // Experience compression and memory update
- 11:    $\mathcal{M}_{t+1} \leftarrow \text{COMPRESS}(\mathcal{M}_t \cup \mathcal{F}_t, M_{\max})$  using Equations
- 12:   // Parameter update
- 13:    $\theta \leftarrow \theta - \eta \nabla_\theta \mathcal{L}_{\text{total}}(\theta)$  using Equations
- 14: **end for**
- 15: **return** trained model  $f_\theta$ , experience memory  $\mathcal{M}_T$

---

$K$ ) and standard query–key–value attention, the total time complexity over  $L$  layers is

$$\mathcal{O}(L \cdot |\mathcal{V}| \cdot (HKd_h + d_h^2 + KC_{LLM})),$$

where  $HKd_h$  accounts for attention score/aggregation,  $d_h^2$  for linear projections, and  $KC_{LLM}$  for contextual LLM prompting per node.

**Theorem 3** (Attention Complexity). *For a graph with  $|\mathcal{V}|$  nodes, maximum degree  $\Delta$ , and  $L$  layers, the time complexity per iteration is:*

$$\mathcal{O}(L \cdot |\mathcal{V}| \cdot K \cdot d_h^2 + |\mathcal{V}| \cdot K \cdot C_{LLM}) \quad (56)$$

where  $C_{LLM}$  is the cost of LLM inference per node pair.

*Sketch.* For each layer and node  $v$ : (i) computing attention scores over  $K$  neighbors with  $H$  heads costs  $\mathcal{O}(HKd_h)$  (dot-products and softmax); (ii) the standard linear projections (e.g.,  $Q, K, V$  and output) contribute  $\mathcal{O}(d_h^2)$  per node; (iii) applying an LLM to each  $(v, u)$  pair for contextual reasoning adds  $\mathcal{O}(KC_{LLM})$ . Summing over  $|\mathcal{V}|$  nodes and  $L$  layers yields the bound. This matches common analyses of attention mechanisms (Vaswani et al. 2017) and message-passing GNNs (Zhou et al. 2020).  $\square$

## Datasets

As illustrated in Table 1, We evaluate on public corpora and synthetic adversarial variants:

- **Enron-Spam:** real enterprise emails labeled ham/spam.
- **Ling-Spam:** linguistic spam dataset.
- **SpamAssassin:** curated spam/ham with headers.
- **TREC 2007/2008 Spam:** realistic benchmarking corpora(Cormack 2007).

Table 1: Dataset statistics.

Dataset	#Emails	Spam(%)	Modalities	Notes
Enron-Spam	33,000	49.3	text+meta	enterprise mix
Ling-Spam	2,893	16.6	text	ling. bias ctrl
SpamAssassin	9,349	56.1	text+meta	rich headers
TREC Spam	75,000	50.0	text+meta+url	realistic dist.
Synthetic-Adv	60,000	50.0	text+meta+url+att	P1–P3 evolving

- **Synthetic-Adversarial:** phases P1–P3 simulating tactic drift (keyword/template, Unicode/leet + domain rotation, AI-generated phishing with forged headers/attachments).

## Experimental Setup

**Baselines.** As elaborated in Table 2, we compare against classical, neural, and graph-based methods:

- **NB / SVM / RF:** TF-IDF + basic metadata(Fette, Sadeh, and Tomasic 2007).
- **TextCNN / BERT:** content-only encoders(Kim 2014).
- **GraphSAGE + MLP**(Hamilton, Ying, and Leskovec 2018): graph topology with shallow features (no LLM attention).
- **Early / Mid Fusion:** concatenation-based multi-modal baselines (input-level vs. intermediate-layer fusion).
- **EvoMail (ours):** heterogeneous email graph + LLM-enhanced COGGNN + self-evolving memory. Ablations: *w/o Context* (remove LLM attention), *w/o Query Optimizer* (static neighbor sampling), *w/o Memory* (no failure-trace memory).

**Evaluation Scenarios.** **Static:** 80/20 train–test split. **Shift:** train on P1; incremental updates on P2–P3 (no revisits), with 10% novel P3 attacks. **Cross-modal:** (1) text-only, (2) text+metadata, (3) full graph (text+metadata+URLs/attachments).

**Metrics.** Accuracy, Precision, Recall, F1, and Precision@K. We further report **STC** (temporal alignment of attention-based evidence traces) and **CIM** (expert-rated explanation coherence/relevance/auditability; 0–1 scale). In dynamic settings, we track update latency and memory compression efficiency.

**Implementation Details.** Results are averaged over 5 runs (different seeds). The LLM attention head is tuned via LoRA(Xin et al. 2024c)(Liu et al. 2024). The top- $K$  optimizer selects  $K \in \{8, 16, 24, 32\}$  on validation. Experiments use NVIDIA A100 (40GB). Additional hyperparameters are in the supplement(Shchur et al. 2019).

## Results and Analysis

### Overall Performance

Figure 2 provides a multi-metric comparison across EvoMail and its ablated variants, as well as representative baselines. Four metrics are reported: overall accuracy, F1-score, structured-temporal consistency (STC), and cognitive interpretability (CIM). Several insights emerge. First, the full EvoMail achieves the highest scores across all metrics, with

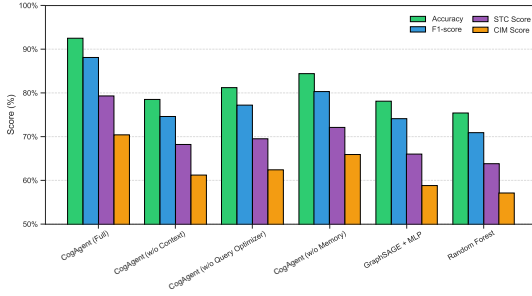


Figure 2: Overall performance comparison across models (NB, SVM, RF, TextCNN, BERT, GraphSAGE+MLP, Fusion baselines, EvoMail). EvoMail consistently outperforms baselines in accuracy, F1, and interpretability (CIM).

Table 2: Overall performance (macro-averaged across datasets). Best in **bold**.

Model	Acc	Prec	Rec	F1	CIM
NB	88.4	84.1	82.7	83.4	0.40
SVM	89.3	85.6	84.7	85.1	0.41
RF	89.7	85.9	85.2	85.5	0.43
TextCNN	90.5	87.1	86.3	86.7	0.45
BERT	92.0	87.8	86.0	86.9	0.52
GraphSAGE+MLP	90.8	87.5	87.2	87.3	0.48
Early Fusion	92.2	88.2	88.6	88.4	0.55
Mid Fusion	92.1	88.0	88.8	88.5	0.56
<b>EvoMail</b>	<b>92.8</b>	<b>89.9</b>	<b>89.3</b>	<b>89.6</b>	<b>0.70</b>

accuracy ( $\approx 93\%$ ) and F1 ( $\approx 89\%$ ) outperforming all baselines, while also delivering superior STC and CIM. Second, removing the LLM context module (*w/o Context*) causes the largest drop—over 14% in F1 and severe degradation in STC/CIM—highlighting the necessity of semantic-structural fusion. Third, excluding the query optimizer or memory module also weakens performance: without the query optimizer, EvoMail loses  $\approx 3$  points in F1 and  $\approx 8$  points in CIM, while the absence of memory reduces interpretability and robustness, showing the benefit of compressing and reusing failure traces. Finally, classical and shallow graph baselines underperform substantially, with GraphSAGE+MLP lagging behind in STC/CIM and Random Forest lowest overall. These results demonstrate that each architectural component adds complementary benefits, and that EvoMail not only improves accuracy but also achieves more robust and regulator-aligned interpretability compared to neural and classical baselines. Table 2 reports aggregate results across corpora. EvoMail attains the best accuracy (92.8%), F1 (89.6%), and interpretability (CIM=0.70). It improves F1 over BERT by +2.7% and over fusion baselines by +1.1%, alongside higher STC.

### Effect of Self-Evolution

Figure 3 tracks F1 performance across ten self-evolution iterations. EvoMail demonstrates a clear upward trajectory,

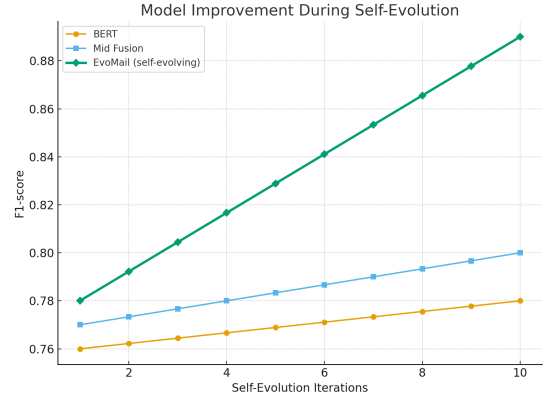


Figure 3: Model improvement during self-evolution iterations. EvoMail shows continuous gains in F1 by reusing failed traces and adversarial examples, whereas static baselines (BERT, Fusion) plateau early with limited improvements.

Table 3: Ablation on EvoMail.

Variant	Acc	Prec	Rec	F1	CIM
Full (EvoMail)	92.8	89.9	89.3	89.6	0.70
w/o Context	83.1	76.0	74.9	75.4	0.44
w/o Query Opt.	92.0	87.0	85.7	86.3	0.62
w/o Memory	90.9	86.4	83.5	84.8	0.58

improving from 0.78 to nearly 0.89 as it reuses failure traces and integrates adversarially generated samples. In contrast, static baselines (BERT and Mid Fusion) show only marginal gains and plateau quickly after a few iterations. This confirms that EvoMail’s red-blue training loop and compressed experience memory enable continual adaptation rather than one-off updates, yielding sustained robustness against evolving attack strategies.

### Ablation Studies

Table 3 quantifies the contribution of each component in EvoMail. The full model achieves the best overall balance across all metrics (Acc: 92.8, F1: 89.6, CIM: 0.70). Removing the LLM attention module (*w/o Context*) leads to the most severe performance degradation, with F1 dropping by 14.2 points and CIM falling below 0.45, underscoring the centrality of semantic-structural fusion. Excluding the query optimizer (*w/o Query Opt.*) also reduces performance (F1: -3.3 points, CIM: -0.08), showing that adaptive neighbor selection is important for capturing relevant evidence. Similarly, discarding the memory module (*w/o Memory*) lowers both F1 (-4.8 points) and CIM (-0.12), highlighting the value of compressing and reusing failure traces for stable adaptation. Overall, each component provides complementary benefits: LLM attention contributes the largest gains in raw accuracy and F1, while query optimization and memory enhance robustness and interpretability, validating EvoMail’s joint design.

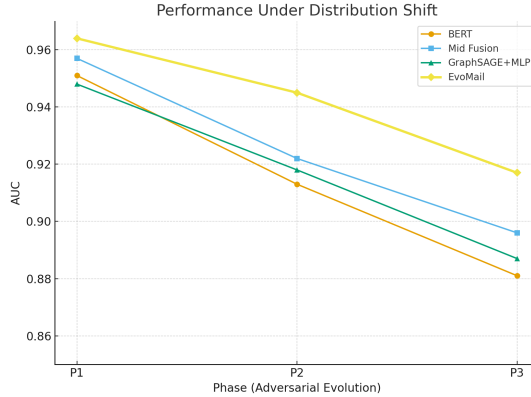


Figure 4: Robustness under distribution shift (Phase 1 → Phase 3). EvoMail sustains the highest AUC and novel-attack F1 across phases, showing stronger adaptability than BERT, Fusion, and GraphSAGE.

Table 4: Shift robustness (AUC across phases;  $\Delta$  is P1–P3). P3 Novel: F1 on 10% unseen attacks.

Model	AUC <sub>P1</sub>	AUC <sub>P2</sub>	AUC <sub>P3</sub>	$\Delta$	P3 Novel
BERT	0.951	0.913	0.881	0.070	76.8
Mid Fusion	0.957	0.922	0.896	0.061	79.4
GraphSAGE+MLP	0.948	0.918	0.887	0.061	78.6
<b>EvoMail</b>	<b>0.964</b>	<b>0.945</b>	<b>0.917</b>	<b>0.047</b>	<b>82.9</b>

## Robustness under Distribution Shift

Figure 4 illustrates the trajectory of AUC across adversarial phases (P1→P3). While all models degrade as spam tactics evolve, EvoMail shows the smallest drop, maintaining an AUC above 0.92 in P3. This stability highlights its ability to generalize across distribution shifts and resist tactic drift(Wang et al. 2025a). In particular, EvoMail not only sustains higher accuracy but also preserves detection quality on unseen attacks, reflecting the benefit of its adversarial self-evolution loop.

Table 4 evaluates performance when attack tactics evolve across phases. EvoMail achieves the highest AUC in all phases (P1: 0.964, P2: 0.945, P3: 0.917), while the degradation from P1 to P3 is the smallest among all models ( $\Delta = 0.047$  vs. 0.061–0.070 for others). This demonstrates that EvoMail adapts more gracefully to distributional drift. Moreover, on novel P3 attacks—emails containing obfuscation patterns not seen during training—EvoMail achieves an F1 of 82.9, substantially outperforming BERT (76.8), Mid Fusion (79.4), and GraphSAGE+MLP (78.6). These results validate the benefits of EvoMail’s self-evolution loop: continuous adversarial generation surfaces unseen tactics, while compressed memory reuse enables the detector to retain and apply knowledge from past failures. Together, these mechanisms reduce the performance erosion typical in static models and sustain robustness in adversarially evolving environments.

Table 5: LLM attention head capacity vs. performance (illustrative).

Config	Params (M)	Acc	F1	CIM
Small	15	91.6	88.1	0.63
Medium	38	92.3	89.1	0.67
Large	76	<b>92.8</b>	<b>89.6</b>	<b>0.70</b>

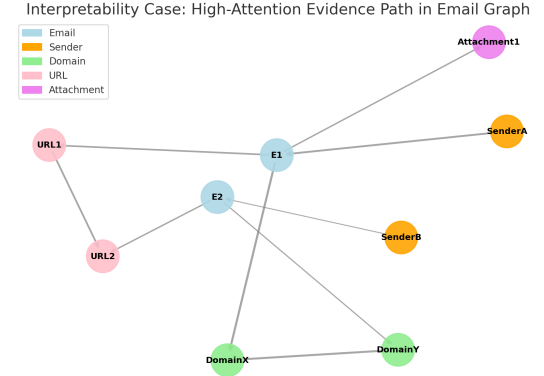


Figure 5: Interpretability case study. The heterogeneous email graph highlights high-attention evidence paths (e.g., suspicious domains, obfuscated URLs, forged headers). EvoMail provides structured audit trails that align with security analyst reasoning.

## Effect of LLM Head Capacity

Table 5 examines the effect of scaling the LLM attention head capacity. As expected, larger configurations yield higher accuracy, F1, and CIM: the small model (15M parameters) achieves 91.6% accuracy and 0.63 CIM, while the large model (76M) reaches 92.8% accuracy and 0.70 CIM. The medium model (38M) already delivers strong performance (92.3 Acc, 89.1 F1, 0.67 CIM), suggesting that EvoMail gains substantial benefits from moderate capacity without requiring very large models. This result highlights a favorable trade-off: while scale improves interpretability and robustness, EvoMail remains competitive even under parameter-efficient settings.

## Interpretability Case Study

To demonstrate how EvoMail produces transparent reasoning, we visualize in Figure 5 a heterogeneous email graph with attention-highlighted evidence paths. Each node corresponds to an entity type (emails, senders, domains, URLs, attachments), and edges denote relations such as `sent-to`, `contains`, and `hosted-on`. High-attention paths reveal the cues that drive the final spam/phishing prediction: for instance, suspicious domains (DomainX/DomainY), obfuscated URLs (URL1/URL2), and a forged attachment–sender linkage. By surfacing these traces, EvoMail provides structured audit trails that closely align with how human security analysts investigate phishing campaigns, bridging detection performance with interpretability(Zhou et al. 2024a).

## Case Study: Obfuscated Phishing Variant

A polymorphic phishing email using zero-width Unicode, forged Reply-To, and a homograph domain evades content-only models. EvoMail elevates attention to SPF failures, URL reputation, and graph anomalies, matching to similar patterns in memory; confidence increases from 0.78 to 0.92 with an interpretable trace (high CIM).

## References

Bach, S.; Binder, A.; Montavon, G.; Klauschen, F.; Müller, K.-R.; and Samek, W. 2015. On Pixel-Wise Explanations for Non-Linear Classifier Decisions by Layer-Wise Relevance Propagation. *PLOS ONE*, 10(7): 1–46.

Brown, T. B.; Mann, B.; Ryder, N.; Subbiah, M.; Kaplan, J.; Dhariwal, P.; Neelakantan, A.; Shyam, P.; Sastry, G.; Askell, A.; Agarwal, S.; Herbert-Voss, A.; Krueger, G.; Henighan, T.; Child, R.; Ramesh, A.; Ziegler, D. M.; Wu, J.; Winter, C.; Hesse, C.; Chen, M.; Sigler, E.; Litwin, M.; Gray, S.; Chess, B.; Clark, J.; Berner, C.; McCandlish, S.; Radford, A.; Sutskever, I.; and Amodei, D. 2020. Language Models are Few-Shot Learners. arXiv:2005.14165.

Chen, Y.; Yangfan, H.; Xuxiang, T. A.; Dong, C.; Jianhui, W.; Tianyu, S.; Arsalan, H.; and Pei, L. 2025. WcDt: World-Centric Diffusion Transformer for Traffic Scene Generation. In *2025 IEEE International Conference on Robotics and Automation (ICRA)*, 6566–6572.

Cormack, G. V. 2007. TREC 2007 Spam Track Overview. In *Text Retrieval Conference*.

Devlin, J.; Chang, M.-W.; Lee, K.; and Toutanova, K. 2019. BERT: Pre-training of Deep Bidirectional Transformers for Language Understanding. arXiv:1810.04805.

Du, Y.; Yang, H.; Chen, M.; Luo, H.; Jiang, J.; Xin, Y.; and Wang, C. 2024. Generation, augmentation, and alignment: a pseudo-source domain based method for source-free domain adaptation. *Machine Learning*, 113(6): 3611–3631.

Ede, T. v.; Aghakhani, H.; Spahn, N.; Bortolameotti, R.; Cova, M.; Continella, A.; Steen, M. v.; Peter, A.; Kruegel, C.; and Vigna, G. 2022. DEEPCASE: Semi-Supervised Contextual Analysis of Security Events. In *2022 IEEE Symposium on Security and Privacy (SP)*, 522–539.

Fette, I.; Sadeh, N.; and Tomasic, A. 2007. Learning to Detect Phishing Emails. In *Proceedings of the 16th International Conference on World Wide Web (WWW '07)*, 649–656.

Ganguli, D.; Lovitt, L.; Kernion, J.; Askell, A.; Bai, Y.; Kadavath, S.; Mann, B.; Perez, E.; Schiefer, N.; Ndousse, K.; Jones, A.; Bowman, S.; Chen, A.; Conerly, T.; Das-Sarma, N.; Drain, D.; Elhage, N.; El-Showk, S.; Fort, S.; Hatfield-Dodds, Z.; Henighan, T.; Hernandez, D.; Hume, T.; Jacobson, J.; Johnston, S.; Kravec, S.; Olsson, C.; Ringer, S.; Tran-Johnson, E.; Amodei, D.; Brown, T.; Joseph, N.; McCandlish, S.; Olah, C.; Kaplan, J.; and Clark, J. 2022. Red Teaming Language Models to Reduce Harms: Methods, Scaling Behaviors, and Lessons Learned. arXiv:2209.07858.

Ghadimi, S.; and Lan, G. 2013. Stochastic first-and zeroth-order methods for nonconvex stochastic programming. *SIAM journal on optimization*, 23(4): 2341–2368.

Goenka, R.; Chawla, M.; and Tiwari, N. 2024. A comprehensive survey of phishing: mediums, intended targets, attack and defence techniques and a novel taxonomy. *International Journal of Information Security*, 23(2): 819–848.

Goodfellow, I. J.; Shlens, J.; and Szegedy, C. 2015. Explaining and Harnessing Adversarial Examples. arXiv:1412.6572.

Hamilton, W. L.; Ying, R.; and Leskovec, J. 2018. Inductive Representation Learning on Large Graphs. arXiv:1706.02216.

He, K.; Zhang, X.; Ren, S.; and Sun, J. 2015. Deep Residual Learning for Image Recognition. arXiv:1512.03385.

Khosla, S.; Zhu, Z.; and He, Y. 2023. Survey on Memory-Augmented Neural Networks: Cognitive Insights to AI Applications. arXiv:2312.06141.

Kim, Y. 2014. Convolutional Neural Networks for Sentence Classification. arXiv:1408.5882.

Kirkpatrick, J.; Pascanu, R.; Rabinowitz, N.; Veness, J.; Desjardins, G.; Rusu, A. A.; Milan, K.; Quan, J.; Ramalho, T.; Grabska-Barwinska, A.; Hassabis, D.; Clopath, C.; Kumaran, D.; and Hadsell, R. 2017. Overcoming catastrophic forgetting in neural networks. *Proceedings of the National Academy of Sciences*, 114(13): 3521–3526.

Li, J.; Du, T.; Ji, S.; Zhang, R.; Lu, Q.; Yang, M.; and Wang, T. 2020. TEXTSHIELD: robust text classification based on multimodal embedding and neural machine translation. In *Proceedings of the 29th USENIX Conference on Security Symposium, SEC'20*. USA: USENIX Association. ISBN 978-1-939133-17-5.

Li, Y.; Li, J.; Liu, X.; and Xu, L. 2025. Deep anomaly detection on attributed networks by graph update. *Computing*, 107(6): 134.

Li, Y.; Xiong, H.; Kong, L.; Bian, J.; Wang, S.; Chen, G.; and Yin, D. 2024. GS2P: a generative pre-trained learning to rank model with over-parameterization for web-scale search. *Machine Learning*, 113(8): 5331–5349.

Li, Y.; Xiong, H.; Kong, L.; Wang, S.; Sun, Z.; Chen, H.; Chen, G.; and Yin, D. 2023a. LtrGCN: Large-Scale Graph Convolutional Networks-Based Learning to Rank for Web Search. In De Francisci Morales, G.; Perlich, C.; Ruchansky, N.; Kourtellis, N.; Baralis, E.; and Bonchi, F., eds., *Machine Learning and Knowledge Discovery in Databases: Applied Data Science and Demo Track*, 635–651. Cham: Springer Nature Switzerland. ISBN 978-3-031-43427-3.

Li, Y.; Xiong, H.; Kong, L.; Zhang, R.; Dou, D.; and Chen, G. 2023b. Meta Hierarchical Reinforced Learning to Rank for Recommendation: A Comprehensive Study in MOOCs. In Amini, M.-R.; Canu, S.; Fischer, A.; Guns, T.; Kralj Novak, P.; and Tsoumakas, G., eds., *Machine Learning and Knowledge Discovery in Databases*, 302–317. Cham: Springer Nature Switzerland. ISBN 978-3-031-26422-1.

Li, Y.; Xiong, H.; Wang, Q.; Kong, L.; Liu, H.; Li, H.; Bian, J.; Wang, S.; Chen, G.; Dou, D.; and Yin, D. 2023c. COLTR:

Semi-Supervised Learning to Rank With Co-Training and Over-Parameterization for Web Search. *IEEE Transactions on Knowledge and Data Engineering*, 35(12): 12542–12555.

Liang, X.; Tao, M.; Xia, Y.; Wang, J.; Li, K.; Wang, Y.; He, Y.; Yang, J.; Shi, T.; Wang, Y.; Zhang, M.; and Wang, X. 2025. SAGE: Self-evolving Agents with Reflective and Memory-augmented Abilities. *Neurocomputing*, 647: 130470.

Liang, Z.; Ding, H.; and Fu, W. 2021. A Survey on Graph Neural Networks for Recommendation. In *2021 International Conference on Culture-oriented Science & Technology (ICCST)*, 383–386.

Lin, Y.; Liu, R.; Divakaran, D. M.; Ng, J. Y.; Chan, Q. Z.; Lu, Y.; Si, Y.; Zhang, F.; and Dong, J. S. 2021. Phishpedia: A Hybrid Deep Learning Based Approach to Visually Identify Phishing Webpages. In *30th USENIX Security Symposium (USENIX Security 21)*, 3793–3810. USENIX Association. ISBN 978-1-939133-24-3.

Liu, D.; Zhao, S.; Zhuo, L.; Lin, W.; Xin, Y.; Li, X.; Qin, Q.; Qiao, Y.; Li, H.; and Gao, P. 2025. Lumina-mGPT: Illuminate Flexible Photorealistic Text-to-Image Generation with Multimodal Generative Pretraining. arXiv:2408.02657.

Liu, T.; Liu, X.; Shi, L.; Xu, Z.; Huang, S.; Xin, Y.; and Yin, Q. 2024. Sparse-Tuning: Adapting Vision Transformers with Efficient Fine-tuning and Inference. arXiv:2405.14700.

Lopez-Paz, D.; and Ranzato, M. 2022. Gradient Episodic Memory for Continual Learning. arXiv:1706.08840.

Lucic, A.; ter Hoeve, M.; Tolomei, G.; de Rijke, M.; and Silvestri, F. 2022. CF-GNNExplainer: Counterfactual Explanations for Graph Neural Networks. arXiv:2102.03322.

Lundberg, S.; and Lee, S.-I. 2017. A Unified Approach to Interpreting Model Predictions. arXiv:1705.07874.

Lyu, Z.; Li, Y.; Zhu, G.; Xu, J.; Vincent Poor, H.; and Cui, S. 2025. Rethinking Resource Management in Edge Learning: A Joint Pre-Training and Fine-Tuning Design Paradigm. *IEEE Transactions on Wireless Communications*, 24(2): 1584–1601.

Metsis, V.; Androutsopoulos, I.; and Palouras, G. 2006. Spam Filtering with Naive Bayes - Which Naive Bayes? In *Proceedings of the 3rd Conference on Email and Anti-Spam (CEAS)*.

Palmer, G.; Parry, C.; Harrold, D. J. B.; and Willis, C. 2024. Deep Reinforcement Learning for Autonomous Cyber Defence: A Survey. arXiv:2310.07745.

Qian, C.; Tang, H.; Yang, Z.; Liang, H.; and Liu, Y. 2023. Can Large Language Models Empower Molecular Property Prediction? arXiv:2307.07443.

Ren, X.; Tang, J.; Yin, D.; Chawla, N.; and Huang, C. 2024. A Survey of Large Language Models for Graphs. In *Proceedings of the 30th ACM SIGKDD Conference on Knowledge Discovery and Data Mining*, KDD '24, 6616–6626. ACM.

Ribeiro, M. T.; Singh, S.; and Guestrin, C. 2016. "Why Should I Trust You?": Explaining the Predictions of Any Classifier. arXiv:1602.04938.

Rossi, E.; Chamberlain, B.; Frasca, F.; Eynard, D.; Monti, F.; and Bronstein, M. 2020. Temporal Graph Networks for Deep Learning on Dynamic Graphs. arXiv:2006.10637.

Schlichtkrull, M.; Kipf, T. N.; Bloem, P.; van den Berg, R.; Titov, I.; and Welling, M. 2017. Modeling Relational Data with Graph Convolutional Networks. arXiv:1703.06103.

Shchur, O.; Mumme, M.; Bojchevski, A.; and Günnemann, S. 2019. Pitfalls of Graph Neural Network Evaluation. arXiv:1811.05868.

Silver, D.; Huang, A.; Maddison, C. J.; Guez, A.; Sifre, L.; van den Driessche, G.; Schrittwieser, J.; Antonoglou, I.; Panneershelvam, V.; Lanctot, M.; Dieleman, S.; Grewe, D.; Nham, J.; Kalchbrenner, N.; Sutskever, I.; Lillicrap, T.; Leach, M.; Kavukcuoglu, K.; Graepel, T.; and Hassabis, D. 2016. Mastering the game of Go with deep neural networks and tree search. *Nature*, 529(7587): 484–489.

Thapa, C.; Tang, J. W.; Abuadbba, A.; Gao, Y.; Camtepe, S.; Nepal, S.; Almashor, M.; and Zheng, Y. 2023. Evaluation of Federated Learning in Phishing Email Detection. *Sensors*, 23(9).

Vaswani, A.; Shazeer, N.; Parmar, N.; Uszkoreit, J.; Jones, L.; Gomez, A. N.; Kaiser, Ł.; and Polosukhin, I. 2017. Attention is all you need. *Advances in neural information processing systems*, 30.

Veličković, P.; Cucurull, G.; Casanova, A.; Romero, A.; Liò, P.; and Bengio, Y. 2018. Graph Attention Networks. arXiv:1710.10903.

Vu, M. N.; and Thai, M. T. 2020. PGM-Explainer: Probabilistic Graphical Model Explanations for Graph Neural Networks. arXiv:2010.05788.

Wan, Z.; Dou, Z.; Liu, C.; Zhang, Y.; Cui, D.; Zhao, Q.; Shen, H.; Xiong, J.; Xin, Y.; Jiang, Y.; Tao, C.; He, Y.; Zhang, M.; and Yan, S. 2025a. SRPO: Enhancing Multimodal LLM Reasoning via Reflection-Aware Reinforcement Learning. arXiv:2506.01713.

Wan, Z.; Wu, X.; Zhang, Y.; Xin, Y.; Tao, C.; Zhu, Z.; Wang, X.; Luo, S.; Xiong, J.; Wang, L.; and Zhang, M. 2025b. D2O: Dynamic Discriminative Operations for Efficient Long-Context Inference of Large Language Models. arXiv:2406.13035.

Wang, L.; Zhang, X.; Su, H.; and Zhu, J. 2024a. A Comprehensive Survey of Continual Learning: Theory, Method and Application. *IEEE Transactions on Pattern Analysis and Machine Intelligence*, 46(8): 5362–5383.

Wang, N.; Bian, J.; Li, Y.; Li, X.; Mumtaz, S.; Kong, L.; and Xiong, H. 2024b. Multi-purpose RNA language modelling with motif-aware pretraining and type-guided fine-tuning. *Nature Machine Intelligence*, 6(5): 548–557.

Wang, X.; Chen, J.; Wang, Z.; Zhou, Y.; Zhou, Y.; Yao, H.; Zhou, T.; Goldstein, T.; Bhatia, P.; Huang, F.; and Xiao, C. 2025a. Enhancing Visual-Language Modality Alignment in Large Vision Language Models via Self-Improvement. arXiv:2405.15973.

Wang, X.; Ji, H.; Shi, C.; Wang, B.; Cui, P.; Yu, P.; and Ye, Y. 2021. Heterogeneous Graph Attention Network. arXiv:1903.07293.

Wang, Y.; He, Y.; Wang, J.; Li, K.; Sun, L.; Yin, J.; Zhang, M.; and Wang, X. 2025b. Enhancing intent understanding for ambiguous prompt: A human–machine co-adaption strategy. *Neurocomputing*, 646: 130415.

Wei, A.; Haghtalab, N.; and Steinhardt, J. 2023. Jailbroken: How Does LLM Safety Training Fail? arXiv:2307.02483.

Wu, Z.; Pan, S.; Chen, F.; Long, G.; Zhang, C.; and Yu, P. S. 2021. A Comprehensive Survey on Graph Neural Networks. *IEEE Transactions on Neural Networks and Learning Systems*, 32(1): 4–24.

Xin, Y.; Du, J.; Wang, Q.; Lin, Z.; and Yan, K. 2024a. VMT-Adapter: Parameter-Efficient Transfer Learning for Multi-Task Dense Scene Understanding. *Proceedings of the AAAI Conference on Artificial Intelligence*, 38(14): 16085–16093.

Xin, Y.; Du, J.; Wang, Q.; Yan, K.; and Ding, S. 2024b. MmAP: Multi-Modal Alignment Prompt for Cross-Domain Multi-Task Learning. *Proceedings of the AAAI Conference on Artificial Intelligence*, 38(14): 16076–16084.

Xin, Y.; Luo, S.; Liu, X.; Du, Y.; Zhou, H.; Cheng, X.; Lee, C.; Du, J.; Wang, H.; Chen, M.; Liu, T.; Hu, G.; Wan, Z.; Zhang, R.; Li, A.; Yi, M.; and Liu, X. 2024c. V-PETL Bench: A Unified Visual Parameter-Efficient Transfer Learning Benchmark. In Globerson, A.; Mackey, L.; Belgrave, D.; Fan, A.; Paquet, U.; Tomczak, J.; and Zhang, C., eds., *Advances in Neural Information Processing Systems*, volume 37, 80522–80535. Curran Associates, Inc.

Xiong, H.; Bian, J.; Li, Y.; Li, X.; Du, M.; Wang, S.; Yin, D.; and Helal, S. 2024. When Search Engine Services meet Large Language Models: Visions and Challenges. arXiv:2407.00128.

Ying, R.; Bourgeois, D.; You, J.; Zitnik, M.; and Leskovec, J. 2019. GNNExplainer: Generating Explanations for Graph Neural Networks. arXiv:1903.03894.

Zhao, J.; Qu, M.; Li, C.; Yan, H.; Liu, Q.; Li, R.; Xie, X.; and Tang, J. 2023. Learning on Large-scale Text-attributed Graphs via Variational Inference. In *The Eleventh International Conference on Learning Representations*.

Zhao, W. X.; Zhou, K.; Li, J.; Tang, T.; Wang, X.; Hou, Y.; Min, Y.; Zhang, B.; Zhang, J.; Dong, Z.; Du, Y.; Yang, C.; Chen, Y.; Chen, Z.; Jiang, J.; Ren, R.; Li, Y.; Tang, X.; Liu, Z.; Liu, P.; Nie, J.-Y.; and Wen, J.-R. 2025. A Survey of Large Language Models. arXiv:2303.18223.

Zhou, J.; Cui, G.; Hu, S.; Zhang, Z.; Yang, C.; Liu, Z.; Wang, L.; Li, C.; and Sun, M. 2020. Graph neural networks: A review of methods and applications. *AI open*, 1: 57–81.

Zhou, Y.; Cui, C.; Yoon, J.; Zhang, L.; Deng, Z.; Finn, C.; Bansal, M.; and Yao, H. 2024a. Analyzing and Mitigating Object Hallucination in Large Vision-Language Models. arXiv:2310.00754.

Zhou, Y.; Fan, Z.; Cheng, D.; Yang, S.; Chen, Z.; Cui, C.; Wang, X.; Li, Y.; Zhang, L.; and Yao, H. 2024b. Calibrated Self-Rewarding Vision Language Models. In Globerson, A.; Mackey, L.; Belgrave, D.; Fan, A.; Paquet, U.; Tomczak, J.; and Zhang, C., eds., *Advances in Neural Information Processing Systems*, volume 37, 51503–51531. Curran Associates, Inc.

Zhuo, L.; Zhao, L.; Paul, S.; Liao, Y.; Zhang, R.; Xin, Y.; Gao, P.; Elhoseiny, M.; and Li, H. 2025. From Reflection to Perfection: Scaling Inference-Time Optimization for Text-to-Image Diffusion Models via Reflection Tuning. arXiv:2504.16080.